Solid Freeform Fabrication 2024: Proceedings of the 35th Annual International Solid Freeform Fabrication Symposium – An Additive Manufacturing Conference
Reviewed Paper

QUANTIFICATION OF RECOATING FORCES IN BINDER JETTING

R. Burger*, V. Leube*, M. Nicklisch* and D. Günther*

*Fraunhofer Institute for Casting, Composite and Processing Technology, IGCV, Garching, Germany 85748

Abstract

Binder jetting in sand has recently become increasingly important for production in additive manufacturing. The performance of this process depends very much on the recoating speed. It is linked to the geometric accuracy of the components. If the recoating speed is too high, individual layers are displaced. The displacement of the component layers is not fully understood. Therefore, the recoating forces must be measured. In this work, the parameters "layer thickness", "recoating speed", "roller speed" and the influence of “printed layers” are measured to validate the suitability of the developed custom measurement device. The values are between 7 mN/cm and 40 mN/cm recoater length. Increasing layer thickness and roller speeds reduce the recoating forces. Increasing recoating speeds increase the recoating forces. Printed areas lead to measurable deviations in the force curves. To reduce the displacement of components, a reduction in the amount of sand used by the recoater is recommended.

Introduction

Sand cores to produce undercuts have been used in the foundry industry for a long time. Concise examples of an industrial application of sand cores are the realization of the internal geometry of a pump housing of molded pumps or the production of the cooling system in combustion engines. The emergence of additive manufacturing technologies in recent decades has strongly increased the geometric freedom in the shaping of these components. In addition to sand cores, sand molds are now also being additively manufactured to produce foundry products. The most common additive manufacturing process for sand cores and sand molds is the binder jetting process. This process is mainly used for complex components in prototype production and for the manufacture of very small and small series, but is rarely used in series production. [1].

Sand-binder jetting has a sand volume capacity of more than 450 l/h and, in combination with casting, it is the most productive process [1, 2]. The three-stage process consists of creating building space, recoating and printing. The critical step in this process chain is recoating. Smoothing the unevenly deposited sand introduces forces into the new layer and the layers below. This results in displacements in the zone of influence of this force, which deforms the component areas that have not yet fully hardened. This leads to unacceptable geometric deviations in the final sand components, which are transferred to the metal components during the casting process. Currently the volume capacity is limited by the speed of the recoating operationg, which leads to an extension of the manufacturing process of the sand components. In industrial applications, for recoating speed no more than 0.3 m/s is parameterized. Recoating speeds above this value do not

result in a stable process and lead to geometric errors. These can only be avoided in complex process analyses and optimizations.

The forces, which causes the geometric deviations, have so far only been investigated in simulations. These simulations are largely limited to manufacturing processes for additively manufactured metal and plastic components, where powder morphology is different to sand-binder jetting [3–5]. In addition, the results of the investigations differ by orders of dimension, so that no reliable conclusions can be drawn about the influence of the coating process, especially regarding sand-binder jetting. The author's aim is to experimentally record the forces acting in the sand powder bed, which have a significant effect on the geometric deviation and to assign them to process parameters for influencing the manufacturing speed.

State of the art

Industrial applications

An important form of additive manufacturing is direct additive manufacturing in which the final component is formed in a single process step. In contrast, in indirect or multi-stage additive manufacturing, the tool is produced in the first step. This determines the geometric shape of the component. In the second step the component is manufactured, and the basic material properties are defined. Indirect additive manufacturing can include more than two steps, see also DIN EN ISO/ASTM 52900:2021 [6]. This process is often more cost efficient in producing larger components than conventional additive manufactoring.

Important additive manufacturing processes in foundry technology are the powder bed fusion (PBF) and binder jetting (BJ-AM) processes. In BJ-AM processes, sand is mainly used as a particle material. Sand cores or sand molds are produced. Sand cores can be assembled as a core package in order to implement complex geometries. This is usually used to reproduce and prepare conventional core shooting. For complex geometric component shapes, entire sand molds are produced in a multi-stage sand-BJ-AM process, which are then further processed in the subsequent sand casting process. The process stages are as follows:

- Lowering: The space for creating another layer is created.
- Recoating: The room is filled with new sand.
- Printing: Selective printing creates localized cohesion between individual sand particles across layers.

These steps are repeated cyclically until the components are finished, as shown in Figure 1.

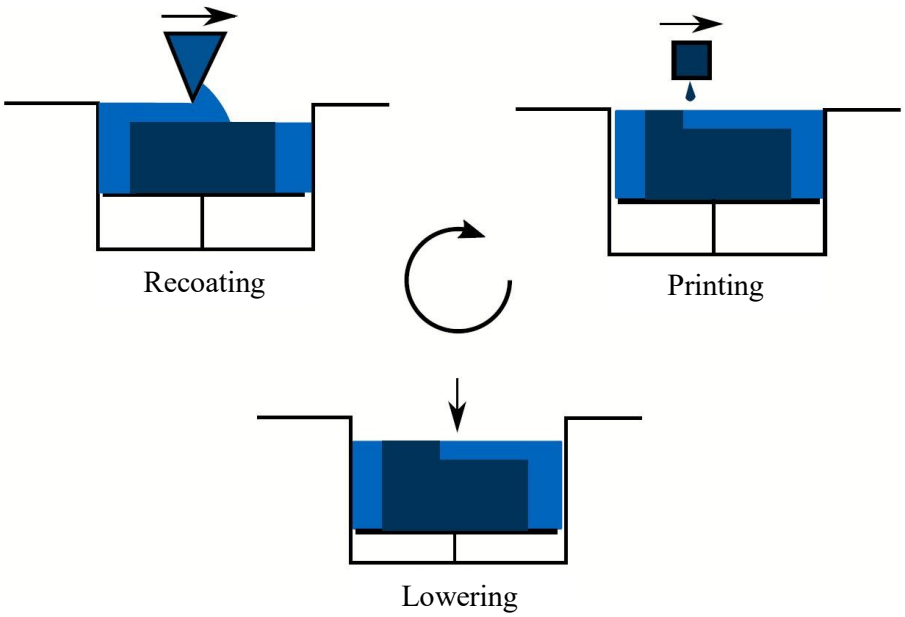

Figure 1: Three-stage process of sand BJ. The steps "lowering" - "recoating" - "printing" are repeated cyclically.[7]

The first process step "lowering" is closely linked to the process parameters for the second process step "recoating". Inkjet printing technology is used in the last process step “printing”. The selective bonding of the powder particles in the BJ-AM takes place via the selective entry of binder liquid and occurs through thermal, chemical or physical reactions.

Recoating forces

In the recoating process as defined above, the first process step involves filling the entire surface of the space created with particle material. This newly created layer must then be smoothed. In BJ-AM processes, powder is usually applied from above. The recoater, which moves with the powder hopper, moves over the build area and releases the powder material. The build area is smoothed mainly at the same time. The type of geometry and its movement have a significant effect on the properties of the powder bed. The powder bed density, the segregation of the particles and their distribution, surface quality and component quality are all influenced. The geometry and speed of the recoater affect the location of the particle flow. According to [4], the particles are distributed either predominantly in the immediate area of the recoater or over the front flank of the powder pile in the recoating direction. The normal forces occurring between the particles and particle velocities are distributed accordingly over the powder roller [4]. The forces that occur depend on the particle size, the recoating gap in relation to the particle size, the recoating speed and the eventually rotational speed of the recoater [5]. Overall, the forces occurring in the recoating direction are of high-frequency [4, 5]. According to consistent studies, the largest force components occur in the x and z directions [3–5].

Particle behavior and interparticle forces

When simulating forces between sand particles, contact forces between the particles are modeled. Shear and normal forces and, in some cases, rolling resistance moments are taken into account. In addition to material parameters, particle size and shape influence the result. [3, 4]

"Force arcs" form between the particles as shown in Figure 2, with a few particles transmitting the majority of the forces via quasi-point contact zones. [4]

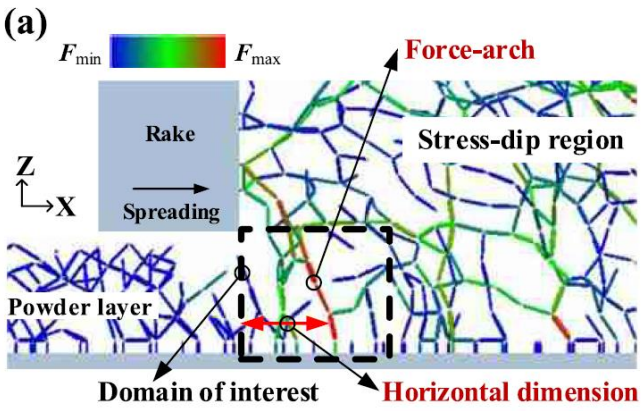

Figure 2: The recoating supports the forces via contact points between the particles via force arcs [8].

These force arcs influence the density of the components [8]. Furthermore, interactions between particles such as adhesion and cohesion influence the flowability and homogeneity of the recoated material [4, 9]. Qualitatively, the described phenomena can be compared across different materials. Due to the influence of material and particle properties, a quantitative classification is only possible on a material-specific basis. Furthermore, these properties influence the velocities in the sand pile upstream of the recoater locally and over time. The forces occurring in the sand pile in front of the recoater are also influenced by underlying layers. Simulations show instantaneous increases in force due to previously printed and thus solidified areas. Parteli et al. show this in the simulation with PA12. They identified a scenario called “crash case” when the roller meets printed area. The simulation of this phenomena is shown in Figure 3. [3]

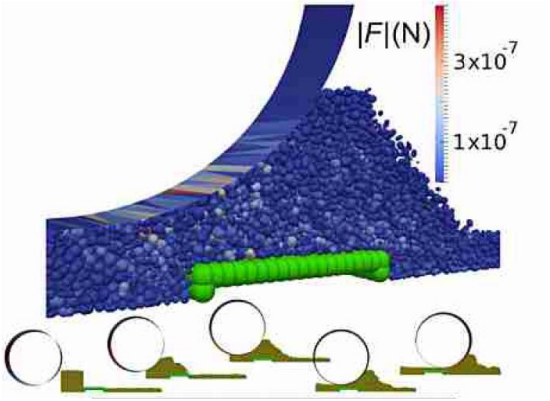

Figure 3: When the roller meets printed areas, so-called crash cases can lead to a local increase in the normal force [3]

During recoating, force peaks occur depending on the particles in the powder bed. The formation also depends on the recoater shape, the recoating speed, the relative speed distribution between the recoater and the build platform and the particle material. Overall, these forces induce shear forces in the powder bed, which lead to layer displacements. [7, 10]

Problem definition

The state-of-the-art shows that there is insufficient research into the sand-BJ-AM process to carry out targeted intervention in the recoating parameters, which are closely related to performance or technology. The main problem are the forces acting between the layers, which lead to geometric defects in the components. Simulations and investigations deal with metallic materials whose properties, processes and parameters cannot be transferred to processes with sand. The relationships between process speeds and the forces between the layers have not been sufficiently investigated. Publications relating to metals predominantly assess the density to increase the sintering potential. This correlation is not relevant for the sand-BJ processes. To the author's knowledge, there are also no published studies of an experimental nature on the forces occurring in the sand-BJ process.

Method

An initial theoretical estimate of the forces to be expected can be made with the help of a model of the local influence zone in front of the recoater. Figure 4 provides an approach for this.

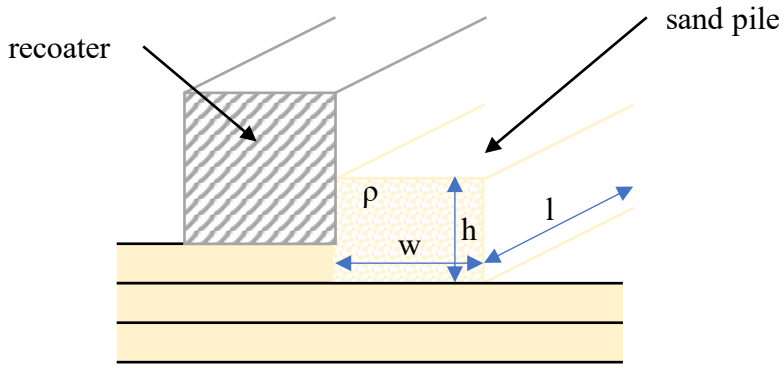

Figure 4: Model to estimate the occurring forces

Figure 4 shows a simplified schematic representation of the recoating process in the influence zone on the powder bed. The theoretical recoating force can be estimated using the sand mass in front of the recoater. The following values, based on industrial plants, are assumed:

- Recoater length *l*: 210 mm
- Width *w*: 10 mm
- Height *h*: 10 mm
- Sand density ρ: 1450 kg/m³

This results in a normal force of 0.3 N acting on the powder bed. With a maximum possible coefficient of friction of 1, this corresponds to a maximum expected force of 0.3 N or 0.014 N/cm recoater length.

Studies on industrial systems show that certain parameter configurations lead to deviations in the component geometry. The components in Figure 5 were produced on a VoxelJet VX1000.

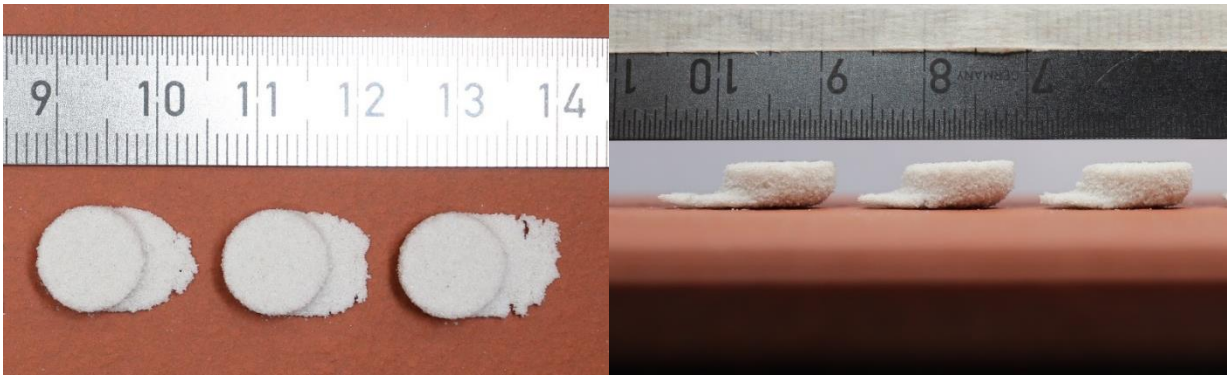

Figure 5: Shifted components with a layer thickness of 280 µm and a recoating speed of 100 mm/s

The test was carried out at standard values. The layer thickness was 280 µm, the recoating speed was 100 mm/s. The evaluations show that the actual cylindrical geometry is shifted in the direction of recoating in the first layers. After more detailed analysis, the cause was narrowed down to the forces acting in the area of the sand pile in front of the recoater.

To describe the forces, these are broken down into the spatial directions and investigated. The first step is to determine the recoating forces in the recoating direction. By varying the process parameters, the influences of these parameters on the process and the forces occurring are investigated. A specially developed measuring device is used for the measurement. The measuring device is installed in an existing test bench, which corresponds in principle to the design of an industrial machine for use in research. The parameters are selected based on industrially used values. The data evaluation is carried out by computer, whereby the filter is used in an independent program.

Test bench

The test bench consists of a machine table on which the components are mounted. The Figure 6 shows the central part of the test bench, while the measuring device is explained in Figure 8. The main components are the three axes for the x, y and z directions. The main parts for printing are located on the x-axis. The build platform, which can be equipped with the measuring device, is installed on the z-axis. A stepper motor is used for positioning.

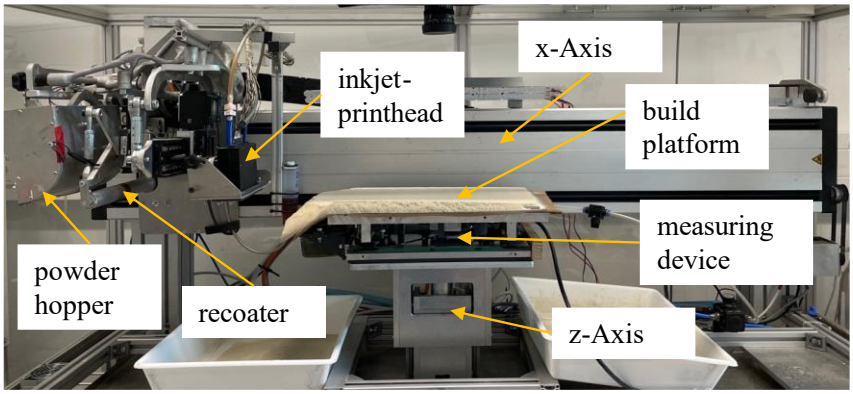

Figure 6: Test bench with main components

The x-axis is a spindle axis with a pitch of 5 mm. The main components of the machine are located on it. These are the powder hopper, recoater, y-axis and the inkjet printhead. A stepper motor with an eccentric is in the powder hopper to improve the delivery of the sand to the build platform. This ensures that the hopper vibrates and is able to spread the sand. The intensity is stepless variable between 0 % and 100 %. The recoater is mounted on a device that allows easy replacement of the recoater. The device is designed for roller and blade. The recoater roller is driven by a stepper motor. The components of the x-axis and the working principle are shown in Figure 7.

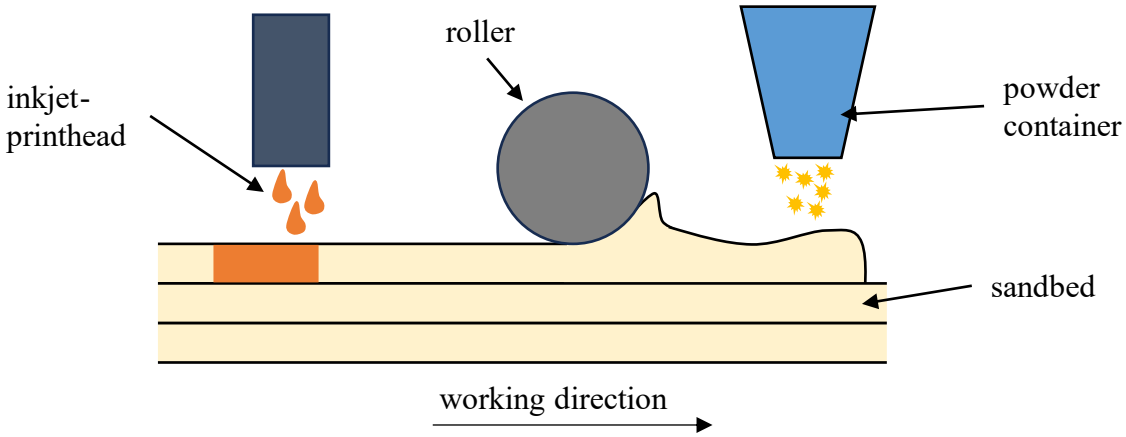

Figure 7: Working principle of the test bench components

The printhead is a Starfire SG 1024 and the binder system used is RPT2 from "Hüttenes Albertus" (HA). The z-axis is fixed via a ball screw and a bearing system. The ball screw is driven by a stepper motor. At the upper end of the z-axis is the build platform, which can be equipped with measuring equipment. Additional measuring devices can be mounted above the construction platform. The entire test bench is controlled via a Beckhoff PLC. It is controlled via a soft PLC called "TwinCAT" and visualization software via computer.

Measurement device

The measurement device for determining the recoating forces is based on the principle of the deflection of a spring. The force acting in the recoating direction is calculated by measuring the displacement and evaluating the equation of motion. The measurement device is shown in Figure 8.

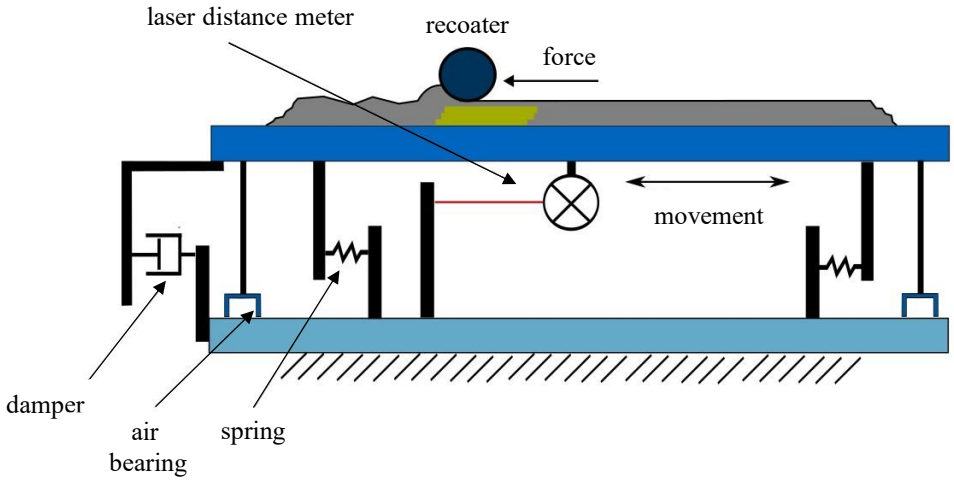

Figure 8: Schematic representation of the measuring device

The base is a glass plate to which plastic blocks are glued. These blocks are used to mount the spring steel wires and as a reference measuring point for distance measurement. The container for the damper is also fixed there. An aluminum plate serves as the base for the build platform. Three air bearings are attached to this. As these are supported on the glass plate with compressed air, the aluminum plate can slide almost frictionless in the x-y plane and is supported by a 3-point bearing in the z-direction. Two spring steel wires are fixed at two points each to fix it in the y-direction and to limit the movement in the x-direction. These are pretensioned and thus determine the spring constant for the system. The design is frictionless and can be regarded as an ideal viscous damper. The damping properties of the system are determined by the fluid in the container. A Keyence LK-H057 is used to measure the distance to determine the displacement of the two plates relative to each other. The technical data can be found in Table 1. The laser is mounted to the aluminum plate and is reflected by a reflector with a diffuse metallic coating located on the glass plate. The laser sensor is controlled via the Keyence LK-G5001P control unit. The data is forwarded to the PLC and synchronized with the position data.

Table 1: Technical data of the Keyence LK-H057 laser

Feature	Value
Reference distance:	50 mm
Linearity:	±10 mm
Repeatability:	± 0,02 %
Scanning cycles:	0.025 µm
Vibration resistance:	10 to 55 Hz, double amplitude 1.5 mm, 2 h in each direction

Data evaluation

The described motion system is evaluated by analyzing the displacement-time function and the Fourier transformation of the impulse response to determine the spring constant and the damping constant, see Figure 9. The calculation is carried out using the formulas for harmonic

oscillations, with the impulse response providing the input data. The evaluation is carried out by approximating an ideal function to the real displacement-time function.

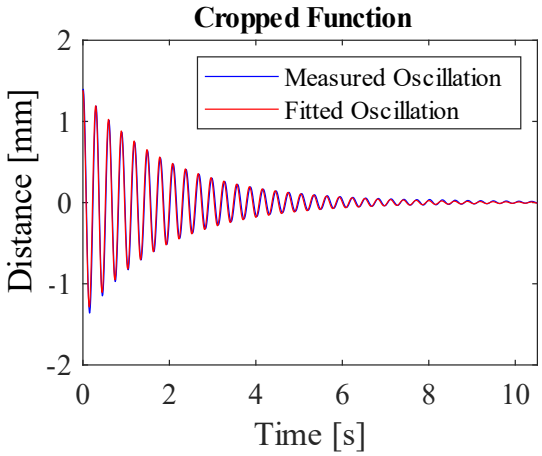

Figure 9: Measured pulse (blue) and ideally calculated function (red)

To verify the spring constant, it is checked independently using the inclined plane method, based on the concept of the sine table. This means tilting the measurement setup to a known angle from horizontal and measuring the displacement of the moving plate. The spring constant is calculated using the downhill slope force and the measured displacement of the moving plate. The method proves to be reliable.

The data is manipulated using an individual digital deconvolution filter. The reason for this is a partial overlap of the eigenfrequency of the measurement setup with the signal. Mathematical filters are used when processing signals that are superimposed with high-frequency oscillations. In dynamic systems, unwanted signal components are separated from the desired ones by identifying their frequencies. Well-known examples of such filters are the low-pass filter and the band-pass filter. User-defined filters are designed to overcome the limitations of classic filters in individual applications. Filters connected in series to eliminate individual frequencies of a measurement chain using an inverse impulse response that was previously determined are referred to as deconvolution filters. [11, 12]

To evaluate filters, their folded step response is examined in the time domain. The critical criterion is the rise time of the step response from 10% to 90% of the impulse response value. Effects that take less time are smoothed by the filter function. Effects to be observed must therefore last longer. In addition, overshoots and long or asymmetrical rises impair the filter behavior. [12]

During inversion of the impulse response in the deconvolution filter, the amplitude of the noise becomes large. The impulse response is therefore Fourier-transformed and convolved with the function, which dampens the noise above a selected frequency, to attenuate the noise. Up to this frequency, the signal remains unaffected by the value "1" in the function. In the transition range, the filter has a rounding effect on the function to avoid an abrupt transition and leading to a leakage effect in the time signal. The inverse impulse responses in the low-pass filter system are plotted in Figure 10.

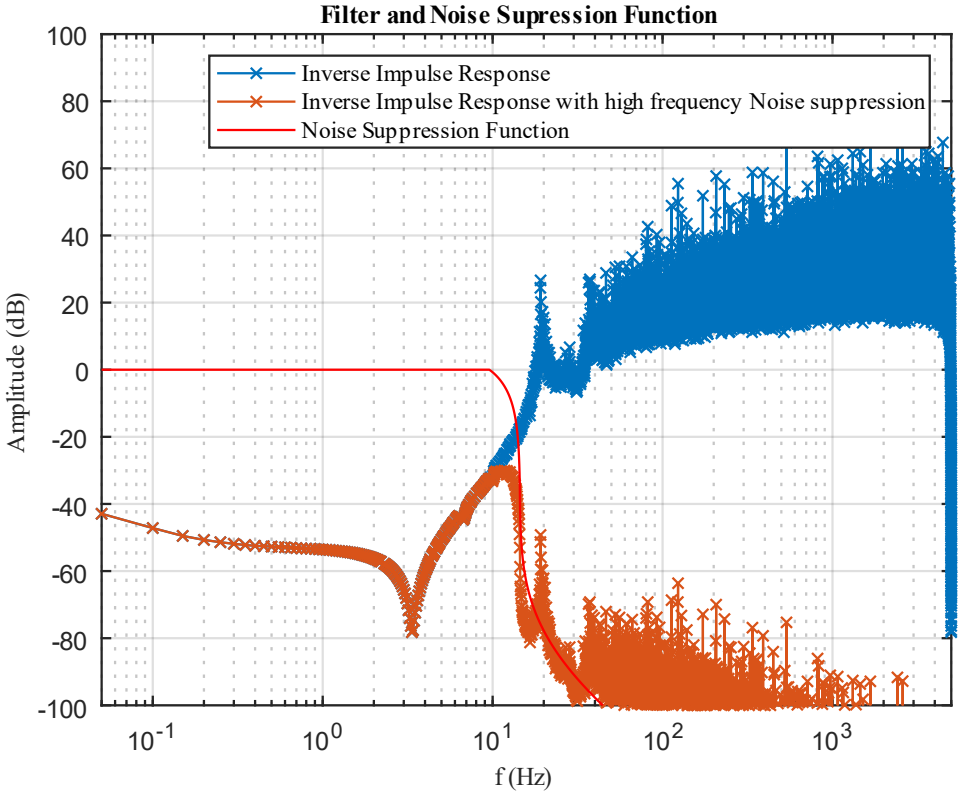

Figure 10: High-frequency filter: The inverse impulse response (blue) is convolved with the low-pass filter (red)

The deconvolution-filter design software converts the impulse response into the frequency domain via a Fast-Fourier-Transformation and inverts it. After attenuating the noise, the impulse response is multiplied by a Hann-Window to reduce leakage effects. The inverse Fast-Fourier-Transformation is used to transform the response back into the time domain. To check the performance of the filter, the deconvolution filter is convolved with a generated step function. The most important characteristic values are checked in a plot, see Figure 11.

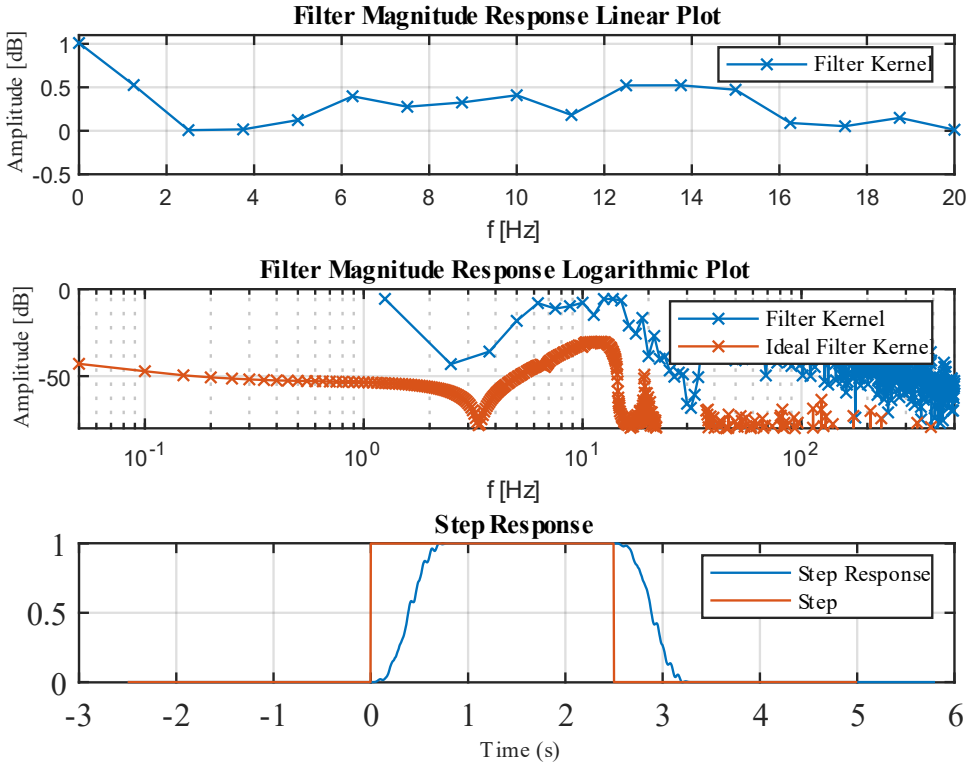

Figure 11: Deconvolution filter performance assessment

The "Magnitude Response Linear Plot" indicates the scaling of statistical values in the 0 Hz range. A good filter function is characterized by an amplitude of 1 dB at 0 Hz. The "Magnitude Response Logarithmic Plot" assesses the qualitative response compared to an ideal filter. The similarity of both responses is a compromise with the rise time of the step response. The "Step Response" comparison provides information about the observability of events. Events that are shorter than twice the rise time have dampened and therefore smaller amplitudes.

Design of Study

A large number of parameters influence the forces. Important parameters are worked out for an initial investigation of the forces occurring between particles and layers. The parameters are shown in Table 2 with the corresponding values.

Table 2: Selection of process parameters for investigating the recoating forces.

Designation	Values	Number of trials
Recoating speed v_R	**100 mm/s**, 300 mm/s, 500 mm/s	> 9 layers
Layer thickness h_L	**280 µm**, 420 µm, 560 µm	> 9 layers
Roller speed v_{Ro}	Counter-rotating: **100 mm/s**, 300 mm/s	18 layers each
Recoater length	210 mm	
Build platform	300 mm x 210 mm	
Gap height in the recoater	2.5 mm	

Vibration of the recoater	70 %	
Sand-binder system	Strobel GS14RP with 0.3 wt.% activator and 3 wt.% binder (HA RPT2)	

The gap height and the vibration intensity in the powder hopper for depositing the sand on the powder bed are not changed in this series of tests. Each test consists of several layers. With a layer thickness of 280 µm, 6 layers are applied and examined per test, with a layer thickness of 420 µm, 4 layers are applied and examined per test, and with a layer thickness of 560 µm, 3 layers are applied and examined per test. Therefore a total thickness of 1.68 mm is printed. This ensures that always the same amount of sand is applied and that the tests are not influenced by the sand mass applied. The individual layers are evaluated. One layer has an area of 300 mm x 210 mm. Sand scraped off the recoater can fall freely from the layer so that the length to be recoated remains the same during the process. The roller speed is to be understood as the unrolled circumference of the roller surface per second.

The force curves that occur are an essential part of the investigations. To compare the tests, the tests should be compared with the standard parameters marked in bold in Table 2. The schematic curves shown in Figure 12 are expected according to the theoretical assumptions.

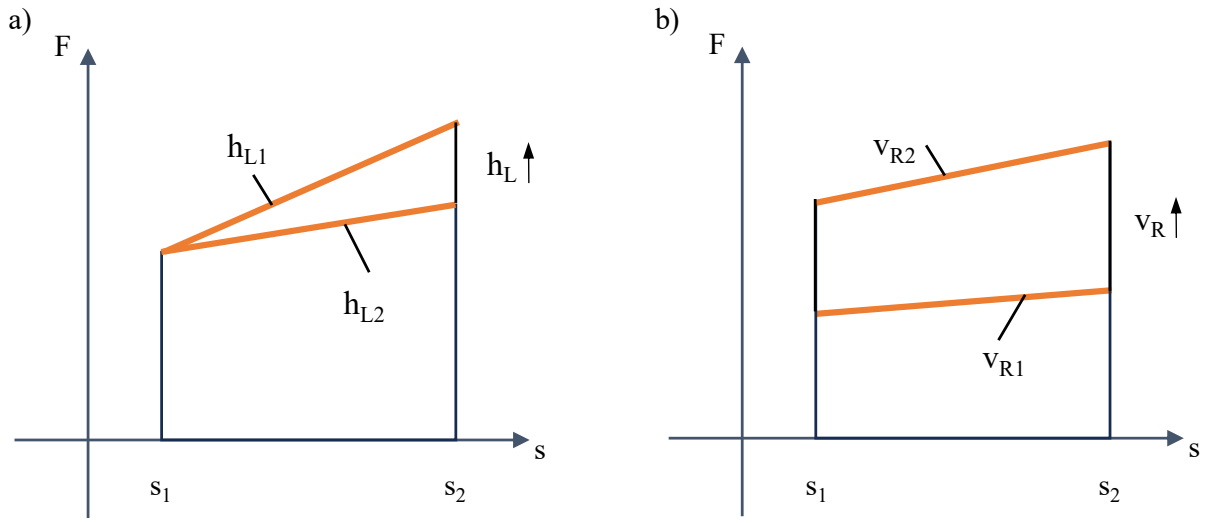

Figure 12: Theoretically expected force curves: Two exemplary force curves with a) increasing layer thickness and b) decreasing recoating speed. The other parameter remains unchanged.

These tests are carried out with variations in the layer thickness and recoating speed parameters. The sand mass deposited remains the same and is optimized for the maximal layer thickness. In the force curves shown above, s_1 represents the roller-sand engagement and s_2 the disengagement of the recoater in the sand bed. The curve a) is expected for the variation of the layer thickness. The experiments are carried out with constant amounts of sand per layer, which means that the amount of sand in front of the recoater increases more with thinner layer thicknesses than with thicker layer thicknesses. It is assumed that the sand can be better distributed due to the larger available volume. Curve b) is expected for the variation of the recoating speed. Due to the

increasing speed at which the recoater hits the powder bed, it is assumed that the force curve is higher overall as the speed increases due to the impulse effect. The same values are expected for the gradient as for the respective coating thicknesses.

In addition, the effect of a printed area is to be investigated. For this purpose, a part of the layer is printed with a rectangle. The configuration is shown schematically in Figure 13.

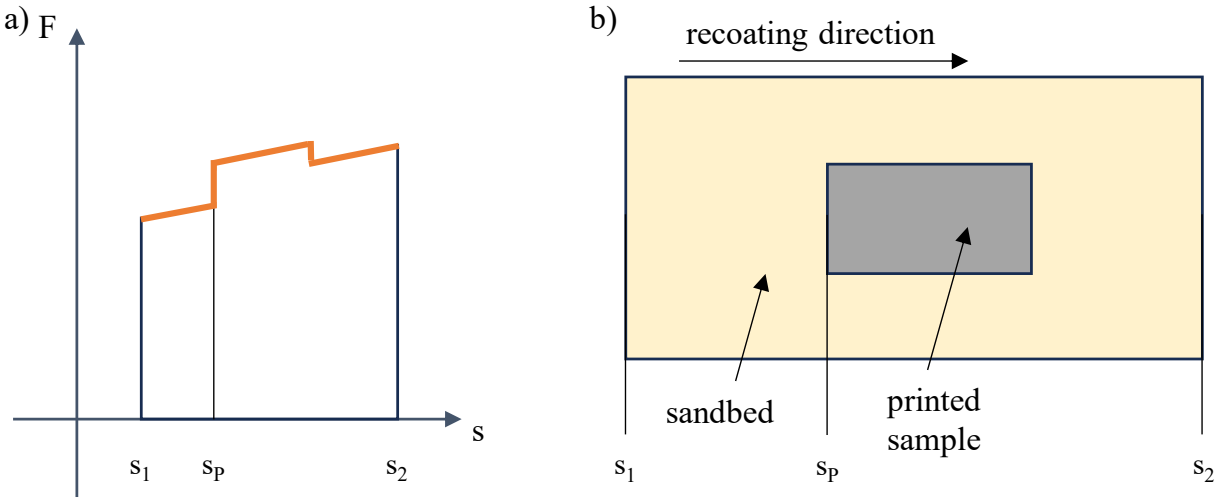

Figure 13: a) Theoretically expected force curve with jump, b) layer with printed component

The test is only carried out with the standard parameters. For the force curve in Figure **13** a), a jump is expected at the point s_P where the printed component begins. This is based on the assumption that printed areas support the force better and therefore more force can be applied to the powder bed. The powder bed is shown in b), where the gray part indicates the printed area. In the recoating direction, the unprinted sand bed is passed over first. The printed component with dimensions of 150 mm x 70 mm is located in the center.

The basic procedure remains the same for all test runs and corresponds to the scheme "lowering" - "applying sand" - "recoating" - "printing". Each test run is repeated three times. The tests are carried out with the standard quartz sand "GS14RP" from Strobel. The average grain diameter is D_{50} = 140 µm. The powder morphology and rheology were taken from previous studies [13]. A measurement device has been designed to measure the forces that occur. A test bench is already available at the institute and replicates a typical machine in an experimental configuration.

Results

The test procedure follows the process described above. This is reflected in the measurement records. The force curves of individual layers are evaluated. An exemplary measurement record is shown in Figure 14.

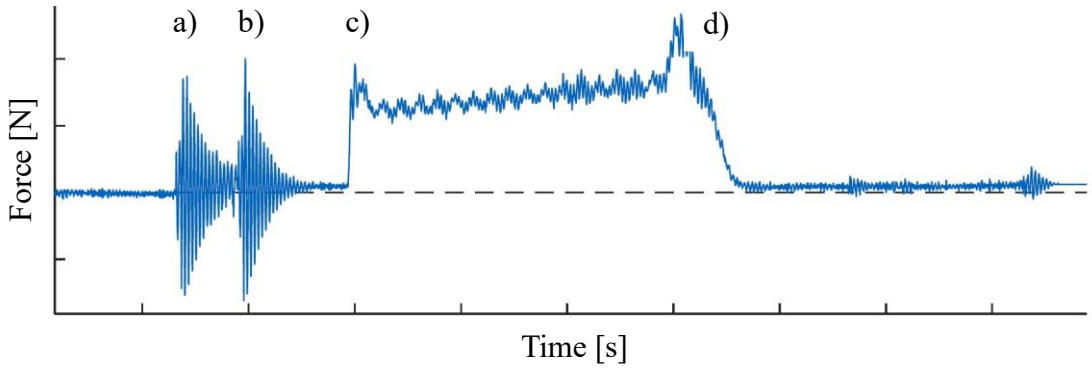

Figure 14: Exemplary measurement record. a) – c): Preparing for recoating, c) – d): Recoating process

Sections a) - d) indicate the following movements:

- a) Starting up and depositing sand: In this process step, the sand is applied unevenly to the construction platform by vibration in the powder hopper during travel in the positive x-direction. A z-distance between the powder hopper and the building platform allows the sand to fall freely and spread.
- b) Motion reversal: The x-axis moves in negative x-direction. The speed up to the end of the measurement corresponds to the recoating speed examined in the parameters.
- c) Engagement of the roller in the powder bed: The roller of the recoater starts recoating.
- d) Roller disengagement: The recoating step is complete, and the axle returns to the starting position.

The peaks in a) and b) represent the movements of the x-axis. Sections c) to d) are interesting for further evaluation. The peak at the start of the measurement at c) represents the impact of the recoater on the sand bed. In the further course, the rotating roller smoothes the powder bed. The force curve is superimposed by an additional oscillation.

Influence of the recoating speed

The tests were carried out at 100 mm/s, 300 mm/s and 500 mm/s and with layer thicknesses of 280 µm, 420 µm and 560 µm. The individual layers are evaluated below. F_{min} refers to the force value at point c) at the time of recoater intrusion with the powder bed. F_{max} refers to the force value at point d) the maximum force value when reaching out of the powder bed. The designations refer to the exemplary measurement diagram in Figure 15.

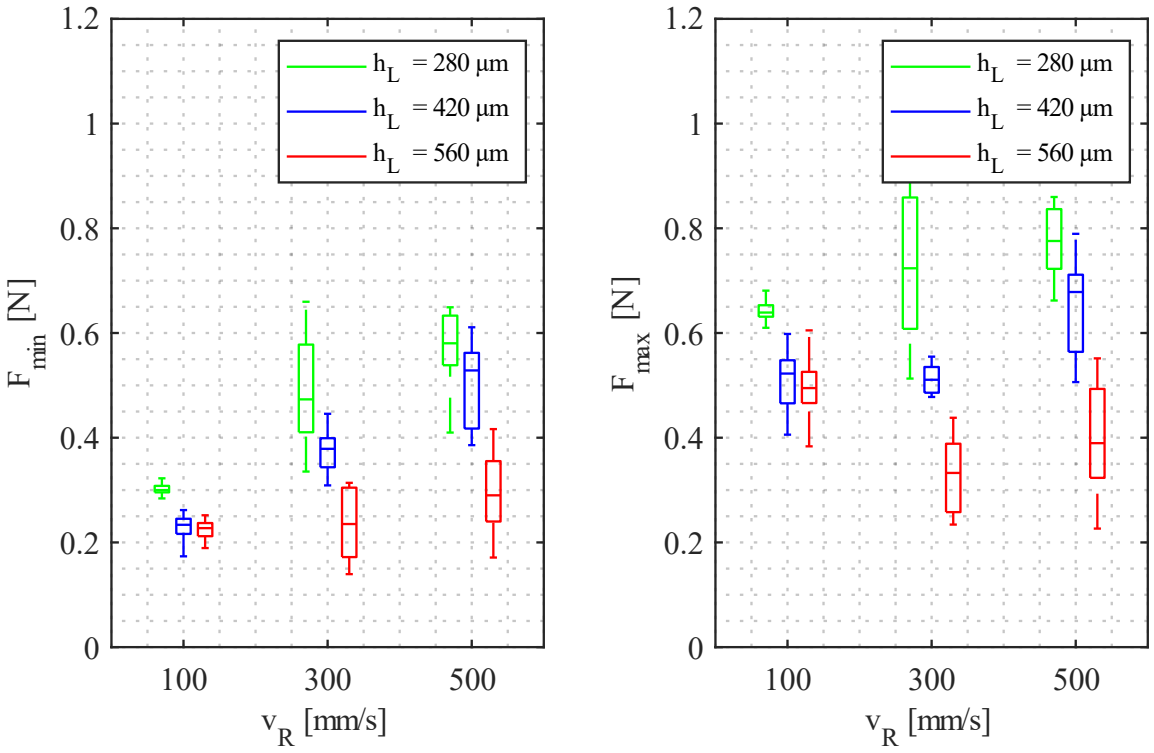

Figure 15: Recoating speed results with minimum forces (left) and maximum forces (right)

Figure 15 shows the minimum and maximum values of the force curves over the different recoating speeds. The tests were carried out for all coating thicknesses investigated. The results show that the forces tend to be lower at higher coating thicknesses. The minimum force tends to increase with lower coating thickness and increasing recoating speed. At higher layer thicknesses, the minimum force increases only slightly with increasing recoating speeds. With regard to the maximum force, no further clear statements can be made in this diagram.

Influence of the layer thickness

The results of the tests from Figure 15 are shown in Figure 16 above the layer thickness. The evaluation is carried out as above.

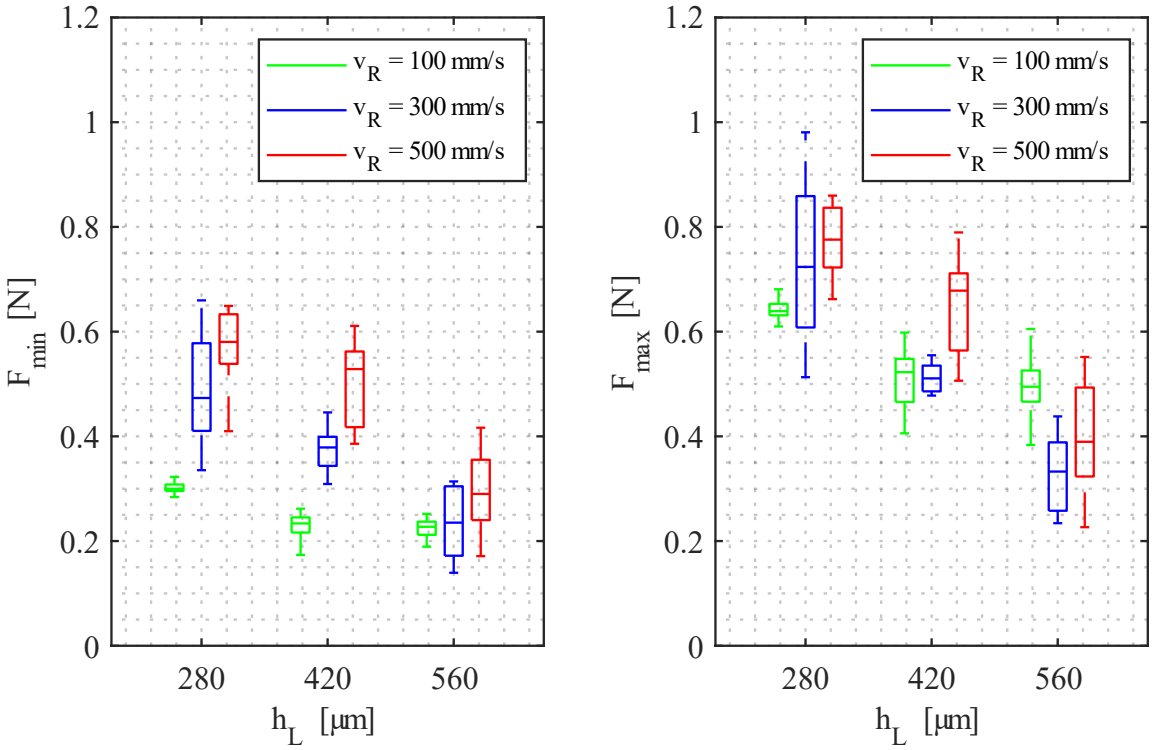

Figure 16: Layer thickness results with minimum forces (left) and maximum forces (right)

This diagram shows that both the minimum and maximum forces decrease with increasing layer thickness. Within a layer thickness, the forces tend to increase with increasing speed.

Evaluation of the force curve

The gradients of the force curves of the results evaluated above are examined below. The tests were carried out at 100 mm/s, 300 mm/s and 500 mm/s and with layer thicknesses of 280 µm, 420 µm and 560 µm. For this evaluation, a regression line is placed in the force curves of the individual layers between points labeled c) and d) in Figure 14.

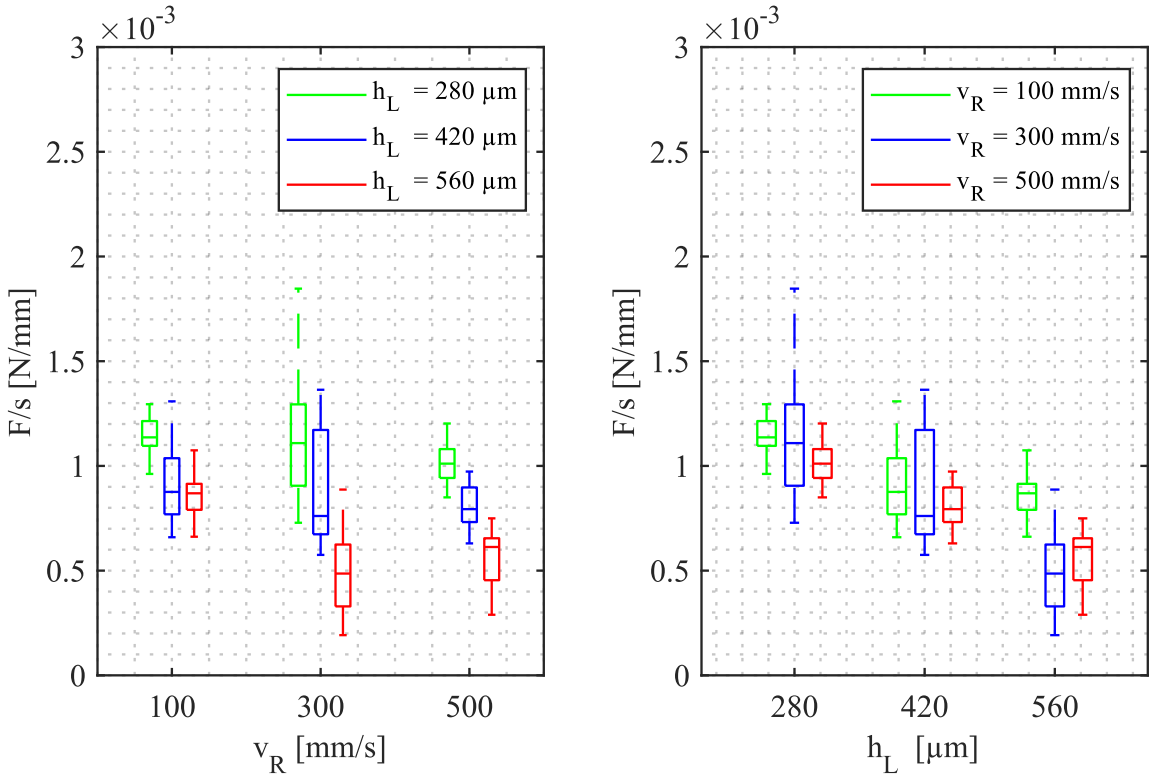

Figure 17: Recoating speed and layer thickness gradients for recoating speed (left) and layer thickness (right)

In Figure 17, the gradients of the regression lines are evaluated. In relation to increasing recoating speeds, the result is not clear. In relation to higher recoating thicknesses, the result tends to be decreasing.

Influence of the roller speed

The tests to investigate the influence of the roller speed were carried out at a coating thickness of h_L = 280 µm and a recoating speed of v_R = 100 mm/s. The results are shown in Figure 18.

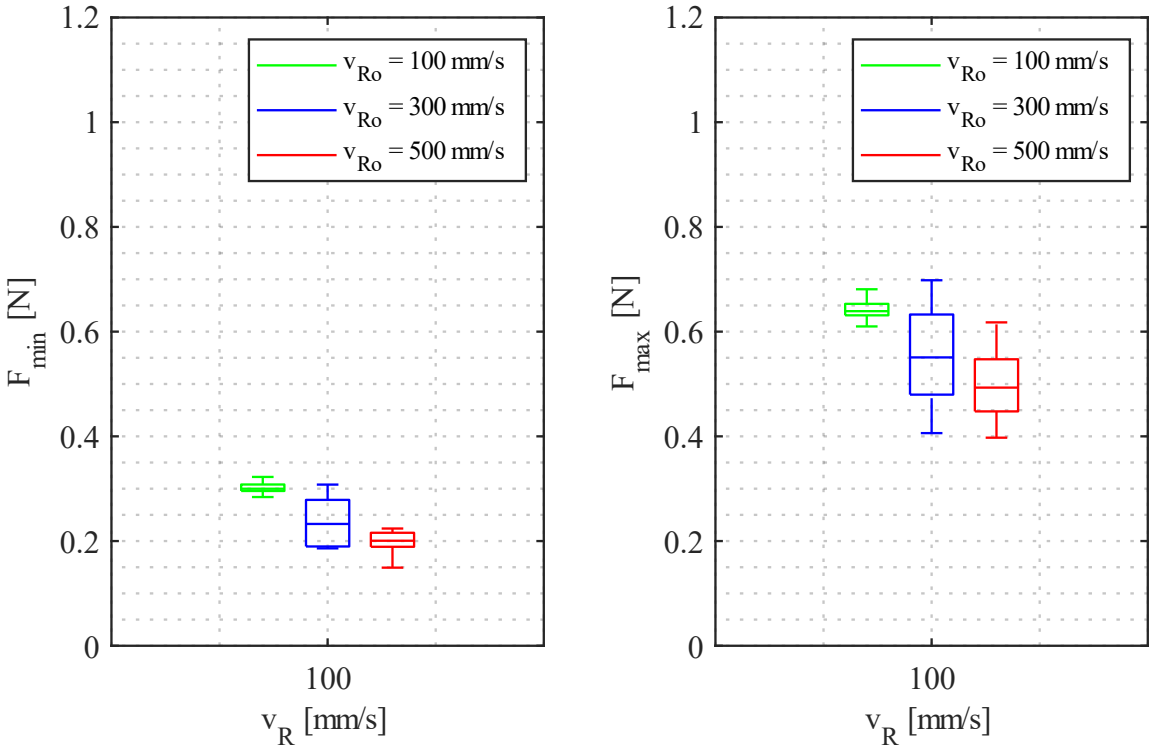

Figure 18: Results of the variation of the roller speed with minimum forces (left) and maximum forces (right)

The roller speed corresponds to the distance unrolled during one revolution per time. An increasing roller speed corresponds to an increase in the relative speed between the roller and the powder bed. The results in the figure above show that both minimum and maximum forces decrease as the roller speed increases.

Influence of a printed area

To observe the difference between printed and unprinted areas, an area of 150 mm x 70 mm is printed on the layer, see also Figure 13. The test is carried out with a layer thickness of 280 µm and a recoating speed of 100 mm/s. The first part of the layer is unprinted. An example of the recorded force curve is shown in Figure 19.

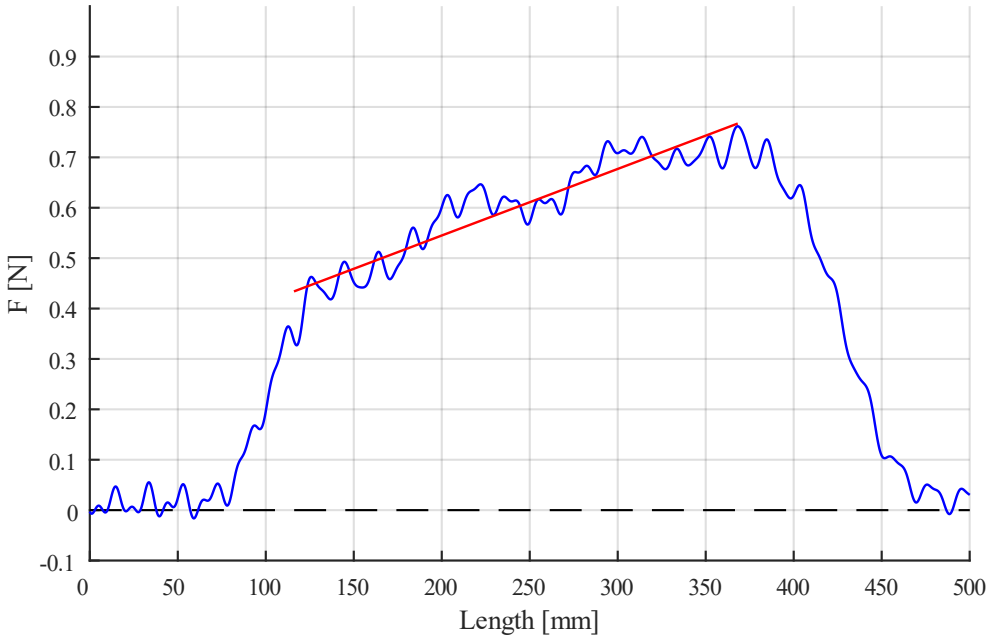

Figure 19: Exemplary measurement record with printed area between 200 mm and 310 mm with local regression line

The Figure 19 shows deviations of the force curve from the mean values at the 200 mm and 310 mm positions. These correspond to the printed area. At the peak, they reach values that are 20 % higher than the average. There is a deviation in the force curve at the point with the printed underlying layer. The force curve rises steeply at the beginning of the printed area. After reaching a local maximum, the force curve approaches the regression line. In the further course over the printed underlayer, the gradient of the force curve increases. This repeats before leaving the printed area. At the end of the layer, the values are again close to the regression line.

The Figure 20 shows the minimum and maximum force as well as the slope of the regression line in comparison with the reference test without printed underlayer.

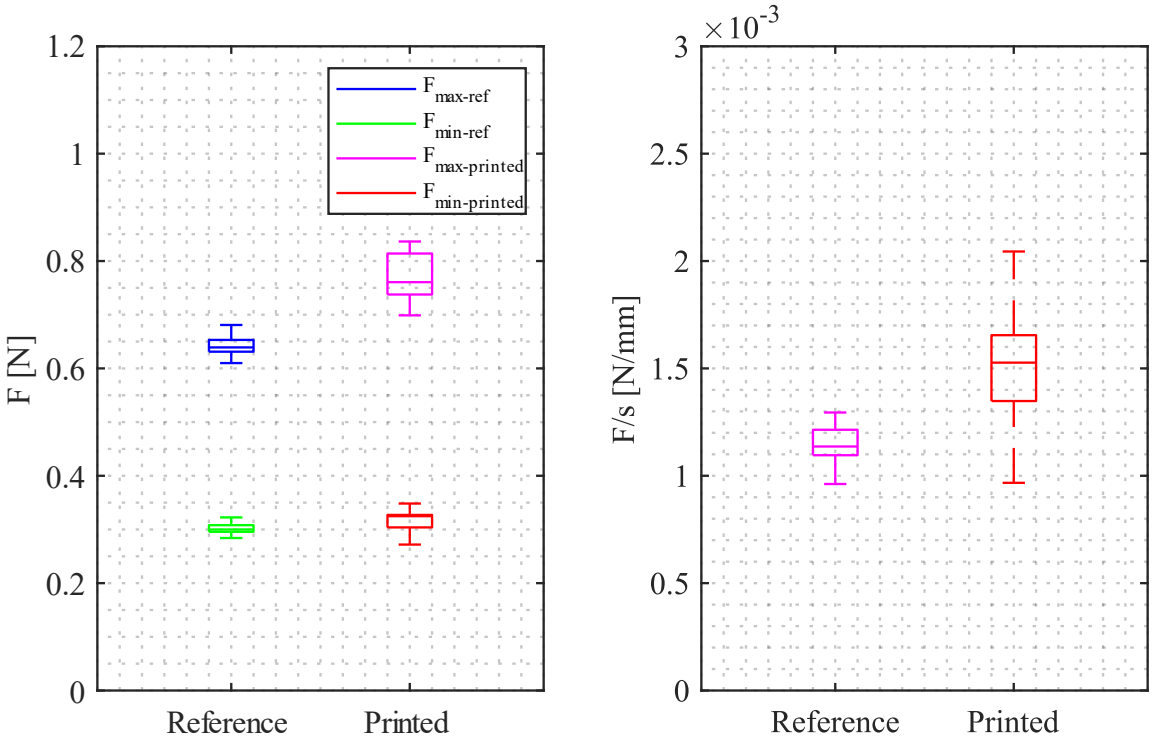

Figure 20: Minimum and maximum force and slope of the regression line for printed component areas

Analysis of the data shows that the force curve up to the printed area behaves in the same way as in the comparative tests. The comparison in the Figure 20 with the reference (same parameters without printed area) shows the same values for the force when the recoater engages in the powder bed. The values when the recoater reaches out of the powder bed are 34.4 % higher with printed areas than in the reference test. The regression line is also steeper overall than in the reference test.

Discussion

So far, only metallic materials as powders have been intensively investigated in the literature. These results show force arcs between the particles in the xz-direction, whereby a large part goes in the z-direction. In this work, the recoating forces in the x-direction were considered, as this is a central task in industrial applications. As these forces have not yet been determined experimentally, a highly sensitive measurement device had to be developed.

Recoating forces were determined experimentally for the first time using an air-bearing measuring system that measures the forces indirectly by means of displacements using a laser. The build platform is mounted "friction-free" and damped by a viscous fluid. Nevertheless, the damping of the system is the target of further optimization. The force was calculated by determining the spring constant by evaluating the impulse response. The eigenfrequency of the developed system lies within the desired measurement spectrum. The measured values are therefore characterized by

strong overlaps. In addition, the force curves must be separated from the oscillations of the natural frequency. The use of a deconvolution filter provided a remedy. The vibrations investigated are above the natural frequency of the measurement setup, which is why the mass acceleration component is significantly included in the force curve. Due to the properties of the measurement setup, further adaptation of the design or optimization of the filter application could be useful.

The tests were carried out in a very practical manner. However, the constant amount of sand across the different layer thicknesses results in a discrepancy with practice. This was accepted for the gain in knowledge.

Regarding the recoating speed, the results show no clear dependencies on the recoating speed for layer-independent sand quantity. The minimum force shows no clear trend. The maximum force increases slightly with decreasing layer thickness. It is noticeable that the recoating speed has no direct correlation with the recoating force and that other factors play an influencing role. In many industrial applications, the amount of sand applied also depends on the recoating speed. At higher recoating speeds, the amount of sand applied therefore decreases, which reduces the normal force on the lower layers.

There is a clear correlation between the coating thickness and the measured force. As the coating thickness increases, the recoating force decreases, both at the point of intrusion and at the point where the recoater emerges from the powder bed. As the total amount of sand applied was designed for high coating thicknesses, this seems logical. The observation of the force curves confirms this assumption.

Varying the roller speed has shown that higher roller speeds lead to lower minimum and maximum forces. As the relative speed increases, more sand is conveyed from the area in front of the roller, which reduces the forces as less sand is "trapped" in the imaginary wedge between the powder bed and the roller. This probably results in a less densely compressed powder bed. It remains to be investigated how a change in the recoating speed and the associated relative speed affects the force curves.

When examining printed areas, changes in the force curve from the reference test were determined. The minimum force when the recoater engages in the unprinted area is comparable to that of the references. As described in Parteli et al. [3], the printed layer could result in a crash, which changes the further course. The force curve over the printed area appears to be superimposed by systemic vibrations. It can be assumed that, due to this phenomenon, the actual force is constantly higher and does not approach the mean values from the unprinted area over the printed area. The sand pile in front of the recoater is likely increase abruptly from the printed area onwards. The maximum value is correspondingly higher. Since there is also a change at the transition to the unprinted area, an influence of the surface chemistry can also be assumed. This theory can have a significant influence on the amount of binder and effects on the component geometry. Printed surfaces also influence the local sand flowability in front of the recoater. The density in the different areas is significantly influenced. This means that printed and unprinted areas react differently to the application of force during recoating.

The study focuses on sand with a particle size of d_{50} = 140 µm. Previous publications are limited to metallic or plastic powders with a smaller grain size. The mechanical effects and

geometric properties, as described in [4], can be transferred to other processes without restriction. In order to interpret the results correctly, further effects such as surface loads must be taken into account for small grain diameters. In addition, process-related characteristics differ depending on the intended application. In the present paper, the sand is applied uniformly to the powder bed, whereas previous studies focus on mechanisms that deposit the entire sand and spread it over the powder bed [4,5,8]. On the one hand, this results in segregation, whereby the particle sizes are unevenly distributed over the powder bed [8]. On the other hand, the powder pile becomes smaller due to the consumption of sand via the powder bed in the mentioned processes, whereas in the present paper the powder pile becomes larger due to excess sand. Overall, the quantification method can be applied to sand-binder jetting without restriction. It can also be applied to other processes to a certain extent by interpreting the respective process characteristics.

Summary and outlook

Experimental determinations of the recoating forces were carried out for the first time using the sand-binder jetting process. It was shown that the designed measurement setup is suitable for the purpose and sufficiently sensitive for measuring the forces. The results provide a good overview of the force flows during recoating. It can be seen that the higher coating thicknesses and lower recoating speeds introduce less force into the powder bed. The data indicates a coupling between the amount of sand in front of the recoater and the speed. In addition, the total force applied over the length of the recoating process is decisive, as the forces add up over the course of the process. Printed areas in the powder bed act as obstacles and increase the force applied during recoating. The results are in good agreement with theoretical considerations and provide important guidelines for action. In order to reduce the displacement of surfaces of a component, the amount of powder in front of the recoater or the normal force exerted by the powder on the powder bed must be minimized. A compromise between displacement and component density must also be sought for systems with a roller.

Further investigations of the recoating forces in the z-direction are necessary for a more precise assessment. These will also provide information on the composition and influence of the shear forces.

References

[1] M. Munsch, M. Schmidt-Lehr, E. Wycisk, and T. Führer, "AMPOWER REPORT 2023: Management Summary," Hamburg, 2023.

[2] ExOne. "Exerial." Accessed: Dec. 19, 2023. [Online]. Available: https://www.exone.com/en-US/3D-printing-systems/sand-3d-printers/exerial

[3] E. J. Parteli and T. Pöschel, "Particle-based simulation of powder application in additive manufacturing," *Powder Technology*, vol. 288, pp. 96–102, 2016, doi: 10.1016/j.powtec.2015.10.035.

[4] L. Wang, A. Yu, E. Li, H. Shen, and Z. Zhou, "Effects of spreader geometry on powder spreading process in powder bed additive manufacturing," *Powder Technology*, vol. 384, pp. 211–222, 2021, doi: 10.1016/j.powtec.2021.02.022.

[5] S. Wu *et al.,* "Study on powder particle behavior in powder spreading with discrete element method and its critical implications for binder jetting additive manufacturing processes,"

Virtual and Physical Prototyping, vol. 18, no. 1, 2023, Art. no. e2158877, doi: 10.1080/17452759.2022.2158877.
[6] *ISO/ASTM 52900:2021, Additive Fertigung – Grundlagen – Terminologie*, DIN EN ISO/ASTM 52900, Deutsche Industrie Norm, 2022.
[7] I. Gibson, *Additive manufacturing technologies,* 3rd ed. Cham: Springer, 2021.
[8] H. Chen, Q. Wei, Y. Zhang, F. Chen, Y. Shi, and W. Yan, "Powder-spreading mechanisms in powder-bed-based additive manufacturing: Experiments and computational modeling," *Acta Materialia*, vol. 179, pp. 158–171, 2019, doi: 10.1016/j.actamat.2019.08.030.
[9] A. Mussatto, R. Groarke, A. O'Neill, M. A. Obeidi, Y. Delaure, and D. Brabazon, "Influences of powder morphology and spreading parameters on the powder bed topography uniformity in powder bed fusion metal additive manufacturing," *Additive Manufacturing*, vol. 38, no. 6, p. 101807, 2021, doi: 10.1016/j.addma.2020.101807.
[10] Y. M. Fouda and A. E. Bayly, "A DEM study of powder spreading in additive layer manufacturing," *Granular Matter*, vol. 22, no. 1, 2020, doi: 10.1007/s10035-019-0971-x.
[11] M. Meyer, *Signalverarbeitung: Analoge und digitale Signale, Systeme und Filter,* 9th ed. (Springer eBook Collection). Wiesbaden: Springer Vieweg, 2021.
[12] S. W. Smith, *The Scientist and Engineer's Guide to Digital Signal Processing // The scientist and engineer's guide to digital signal processing,* 2nd ed. San Diego, Calif.: California Technical Pub, 1999.
[13] M. Schneider *et al.,* "Modelling the microstructure and computing effective elastic properties of sand core materials," *International Journal of Solids and Structures*, vol. 143, pp. 1–17, 2018, doi: 10.1016/j.ijsolstr.2018.02.008.